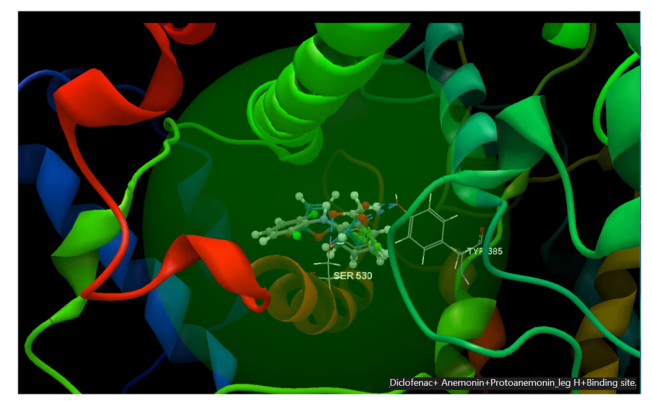
Research Article

Lucia Pirvu*, Amalia Stefaniu, Georgeta Neagu, Lucia Pintilie

Studies on Anemone nemorosa L. extracts; polyphenols profile, antioxidant activity, and effects on Caco-2 cells by in vitro and in silico studies

https://doi.org/10.1515/chem-2022-0137 received January 11, 2022; accepted February 13, 2022

Abstract: In this study, two polar extracts (aqueous and ethanolic) from the aerial part of Anemone nemorosa L. (dried plant) were assessed to reveal their polyphenols profile, antioxidant activity, cytotoxic, and antiproliferative activity on Caco-2 (ATCC-HTB-37) cell line. In silico studies on two key compounds, protoanemonin and anemonin, on four molecular targets - cyclooxygenase-1 and cyclooxygenase-2, and human tankyrase 1 and human tankyrase 2 in relation to human colon cancer cell development have also been achieved. The results are as follows: caffeic acid esters and quercetin glycosides, including (iso) rhamnetin derivates, are the major polyphenol compounds in wood anemone polar extracts; the two polar extracts indicated very strong antioxidant activity in the interval from 0.1 to $5\,\mu g$ [GAE] per $1\,mL$ sample (IC₅₀ < 0.290 μg GAE/mL), and in vitro studies on Caco-2 cells have revealed their simultaneous stimulatory and protective activity exactly in the concentration area with the strongest antioxidant activity. In silico studies have revealed



Graphical abstract

moderate inhibitory activity of the two key compounds, anemonin and protoanemonin, on the four molecular targets studied; it was concluded having particular benefits of the wood anemone polar extracts in managing postoperative intestinal recovery, and generally in regenerative medicine.

Keywords: wood anemone extracts, cell viability, antiproliferative, COX1 and COX2, TNKS1 and TNKS2

Amalia Stefaniu: Department of Pharmaceutical Biotechnologies, National Institute of Chemical Pharmaceutical Research and Development, 112 Vitan Av., Sector 3, Bucharest, Romania; Department of Pharmacology, National Institute of Chemical Pharmaceutical Research and Development, 112 Vitan Av., Sector 3, Bucharest, Romania

Georgeta Neagu: Department of Pharmacology, National Institute of Chemical Pharmaceutical Research and Development, 112 Vitan Av., Sector 3, Bucharest, Romania

Lucia Pintilie: Department of Synthesis, Bioactive Substances and Pharmaceutical Technologies, National Institute of Chemical Pharmaceutical Research and Development, 112 Vitan Av., Sector 3, Bucharest, Romania

1 Introduction

Anemone nemorosa L. (Ranunculaceae family), commonly known as wood anemone or windflower, is an early-spring perennial flower originating from continental Europe, also found in the UK and West Asia [1]. The species in the Ranunculaceae family are classified as toxic plants, for example, buttercups (Ranunculus spp.), anemones (Anemone spp.), hellebores (Helleborus spp.), and Traveller's Joy (Clematis spp.) species [2]. The skin contact with them produces irritant (vesicant) effects, while their ingestion is potentially lethal for herbivores and humans [3]. According to known data, the internal effects

^{*} Corresponding author: Lucia Pirvu, Department of Pharmaceutical Biotechnologies, National Institute of Chemical Pharmaceutical Research and Development, 112 Vitan Av., Sector 3, Bucharest, Romania, e-mail: lucia.pirvu@yahoo.com

Figure 1: Transforming ranunculin into protoanemonin and anemonin.

appear in a few minutes from the time of ingestion rendering to augmented throat inflammation, stomach pain, acute gastroenteritis, and diarrhea mixed with blood, cracked tongue, bleeding cornea, and even narcotic and lethal effects, depending on the doses ingested [3]. The irritant and poisoning effects, both are due to the presence of protoanemonin, a 5-methylidenefuran-2-one lactone type of coumarin, also known as anemonol or ranunculol. Protoanemonin is synthesized through the enzymatic hydrolysis of the glucoside derivate namely ranunculin when the plant is injured by the herbivores and other natural aggressors [4]. As a physical-chemical aspect, protoanemonin is a volatile and highly unstable molecule that spontaneously dimerizes into anemonin (Figure 1). The stable dimer form anemonin, as well as the glucoside form ranunculin, are known as non-toxic compounds [5].

However, species in the *Ranunculaceae* family are attributed with interesting therapeutic applications. British Columbia *Materia Medica* [1], Traditional Chinese Medicine (TCM) *Materia Medica* [4], and homeopathy treaties – all contain numerous data about buttercup's human use, pharmacological activity, doses, and cautions too.

Generally, the older treaties recommend the use of fresh products, therefore they are based on the activity of the toxic compound protoanemonin. According to a feasibility study in 2013 regarding the nonclinical safety of homeopathic preparations, using the example of protoanemonin in Pulsatilla pratensis L., [6] "protoanemonin is classified as a Cramer class III compound with the threshold of toxicological concern (TTC) of 180 µg/day in adults." Also, studies ref. [6] pointed out that "neither computer-aided toxicology methods (Toxtree and Derek Nexus[®]) nor a literature search revealed any evidence of genotoxic, carcinogenic, or teratogenic potential of protoanemonin." As per the principle of homeopathy, a small amount of toxic compound can trigger bodily secretions and stimulate the organs' activity, thus promoting the revival and healing of the damaged tissues, while

larger quantities can induce toxic effects, paralysis, and even death. The homeopathic products from the wood anemone are described as "effective in the treatment of stomach-related disorders and pains, whooping cough, asthma attack in adults as well as children, for skin irritation, and pain in the joints after a high fever [7]."

Regarding the mechanism of toxic effects, some older scientific studies on protoanemonin have revealed that doses of 10⁻³ M produced the disappearance of the mitochondria in the roots of Zea mays, at the same time induced injurious effects on the nuclear, cytoplasmic, and vacuolar structures of the root tissue; the effects on the mitochondria occurred at a concentration level lower than that affecting other cellular organelles, therefore it was concluded that mitochondria damages are the most probable cause of the poisoning effects of protoanemonin in herbivores and humans [8]. More recent pharmacological studies [9] confirmed protoanemonin's ability to cause an energy deficiency in the mitochondria, which is considered a key factor in the function of the heart and skeletal muscle. Specifically, it was proved that protoanemonin may induce "a systemic mitochondrial cytopathy by affecting oxygen availability, substrate oxidation, mitochondrial ATP production, and ATP transfer to the contractile apparatus, via creatine kinase pathway."

Concerning the human health use and benefits, the toxic compound protoanemonin proved antimicrobial, anti-malarial, and antifungal effects against *Staphylococcus aureus*, *Micrococcus lysodeikticus*, *Mycobacterium tuberculosis* var. *Hominis*, *Bacillus subtilis*, *Klebsiella pneumonia*, *Pseudomonas aeruginosa*, *Proteus vulgaris*, *Shigella dysenteriae*, *Trichophyton purpureum*, *Epidermophyton floccosum*, *Candida albicans*, *Rhodotorula glutinis*, and *Saccharomyces cerevisiae* strains [10–13].

The nontoxic compound, anemonin, has been proved with numerous pharmacological activities such as analgesic, spasmolytic and sedative activity, anti-arthritis, antitumor, anti-inflammatory, cardiovascular and neuroprotective DE GRUYTER Studies on A. nemorosa L. extracts — 301

activity. For example, the neuroprotective activity was attributed to antioxidant, and antiapoptotic effects and they were explained by low molecular weight and the proper polarity which makes possible anemonin penetration through the blood-brain barrier. Brain protective effects of anemonin were provided by in vivo studies on rats with nerve injury by ischemia and reperfusion; 90 minutes after the administration of anemonin in rats, it was measured a brain-plasma distribution coefficient value of 0.7, thus proving its certain bioavailability [14,15]. Anemonin compound also proved the capacity to inhibit the synthesis of melanin in skin, specifically by decreasing the mRNA synthesis of tyrosinase-related proteins in melanocytes [16].

This study aims to analyze the polyphenol profile, antioxidant activity, and *in vitro* cytotoxic and antiproliferative activity on Caco-2 cells of two series of highly diluted polar extracts (aqueous and ethanolic) from the aerial part of wood anemone (*A. nemorosa* L.), specifically from the dried plant material. *In silico* docking studies on anemonin and protoanemonin key compounds in anemones, tested on several molecular targets associated with intestinal inflammation and intestinal tumorigenesis in humans have also been achieved; the molecular targets selected for *in silico* study were the two cyclooxygenases, COX-1 and COX-2, and the two human tankyrases, TNKS1 and TNKS2.

2 Experimental procedure

2.1 Materials

2.1.1 Plant material description

The plant material (*A. nemorosa* L. *herba et* flores) was collected in April 2021 from the Romanian sub-Carpathian region, Prahova. Taxonomic identification has been done by the botanist's team of the National Institute for Chemical-Pharmaceutical Research and Development, ICCF, Bucharest, Romania. A voucher specimen is deposited in ICCF *Plant Material Storing Room*; the fresh material was dried at 40°C for three days, afterward, the dried plant was ground to a fine powder (ICCF, deposit Ane16).

2.1.2 Vegetal extracts preparation

Two charges (50 g) of plant powder were extracted with 500 mL of distilled water and 70% ethanol (v/v), under reflux (1 h); the two filtered extracts (Aqueous (whole)

extract series 1 (Anag1) and Ethanolic (whole) extract series 2 (Anet2)) were evaluated as qualitative (polyphenols profile) and quantitative (total phenols) aspects. About 100 mL of each Anaq1 and Anet2 were vacuum concentrated, the residues were solved into 50 mL of acidic solution (4 N HCl), after that hydrolyzed under reflux (30 min). The hydrolyzed samples were (separately) extracted with ethyl acetate solvent (50 mL), three times serially. Each series of three ethyl acetate extracts were vacuum concentrated, and the residues were redissolved into 70% (v/v) ethanol to a final volume of 10 mL sample; the hydrolyzed samples (the hydrolyzed extract obtained from Anag1 (Anh1) and the hydrolyzed extract obtained from Anet2 (Anh2)) were analyzed as concerning qualitative aspects (polyphenol aglycones profile). Other 100 mL of aqueous (whole) extract series 1 (Anaq1) and ethanolic (whole) extract series 2 (Anet2) basic extracts were vacuum concentrated, and the residues were solved into 40% (v/v) ethanol to achieve the punctual 5 mg total phenols expressed as gallic acid equivalents [GAE] per 1 mL sample; the resulting standardized 40% ethanolic extracts (the standardized extract in 40% ethanol (5 mg GAE/mL) from Anaq1 (An1) and the standardized extract in 40% ethanol (5 mg GAE/mL) from Anet2 (An2)) were used in the in vitro studies.

2.1.3 Chemicals, reagents, and references

Chemicals, reagents (e.g., *Folin-Ciocalteau*, *Natural Product*), solvents (e.g., ethanol, ethyl acetate, methanol, chloroform, formic acid, and glacial acetic acid), and the reference compounds (ref.) in analytical studies, e.g., quercetin-3-*O*-galactoside/hyperoside (>97%), quercetin-3-*O*-rutinoside/rutin (min 95%), apigenin-7-*O*-glucoside/cosmosiin (>97%), apigenin-8-*C*-glucoside/vitexin (>96%), apigenin (97%), kaempferol (95%), caffeic acid (99%), chlorogenic acid (>95%), gallic acid (95%), protocatechuic acid (97%), rosmarinic acid (>99%), as well as the cell culture reagents Dulbecco's modified essential media, and fetal bovine serum (FBS) were purchased from Sigma-Aldrich in Romania.

2.2 Experimental design

2.2.1 Chemical quantitative assay

Studies were performed using *Folin Ciocalteau* reagent, the standard method in *Romanian Pharmacopoeia* (FRX) [17]. The results were expressed as gallic acid equivalents, mg [GAE]/1 mL sample ($R^2 = 0.9890$).

2.2.2 Chemical qualitative assay

Chemical qualitative analyses intended the studying of polyphenol's profile in samples. Studies were performed using (HP)TLC method, and two thin layer chromatography protocols [18,19]; system A setting study (ethyl acetate-glacial acetic acid-formic acid-water/100:12:12:26) for polyphenols glycosides assessment, and system B setting study (chloroform-glacial acetic acid-methanol-water/ 64:32:12:8) for polyphenols aglycones assessment, as described in the author's work [20].

2.2.3 Antioxidant activity assay

Antioxidant activity studies were done on the two standardized extracts (5 mg [GAE]/1 mL sample), An1 and An2, prepared as 40% ethanol solutions; each extract was prepared as ten dilution series: $\times 1$, $\times 5$, $\times 10$, $\times 50$, $\times 100$, $\times 200$, $\times 300$, $\times 400$, $\times 500$, $\times 1,000$. The antioxidant activity assay has been done by chemiluminescence (CL) method, luminol $-H_2O_2$ system, pH = 8.6 [21]. Briefly, aliquots of 50 µL of the test sample (dilution point series respectively) were mixed with 200 μL of 10⁻⁵ M luminol (prepared in DMSO), 700 µL 0.2 M tris-HCl pH 8.6 (prepared in bi-distilled water) and 50 µL 10⁻³ M H₂O₂ (also prepared in bi-distilled water). In parallel, the reference sample series, 40% ethanol solvent series respectively, has also been done. CL reaction intensity at each 5s, along with 60 s total time (measured as arbitrary units, a.u.), test sample series versus reference sample series (triplicates) were registered. The analysis of a.u. dynamic, reference sample versus test sample, along with the 60 s, gave information about the antioxidant activity/potency of the test samples, while the comparison of a.u. series along the punctual concentrations in the dilution series allows the estimation of the IC₅₀ values. Finally, IC₅₀ values are were evaluated in comparison with relevant reference compounds (ref.) and other plant extracts.

2.2.4 In vitro pharmacological studies

Starting from the literature data pointing out the stimulatory and protective effects of the plant-derived products from Ranunculacecea family, the present in vitro pharmacological studies were designed to assess the capacity of the polar extracts from dried A. nemorosa plant material to interfere with the activity of the human Caco-2 (ATCC-HTB-37). Studies were done by CellTiter 96 AQueous One Solution Cell Proliferation Assay (MTS) test, and they

were planned to assess cytotoxic and antiproliferative potency of An1 and An2 standardized extracts in the concentration area resulted in the highest antioxidant potency in CL studies. Specifically, two test samples, An1 and An2, were prepared as dilution series: $\times 1$, $\times 5$, $\times 10$, $\times 50$, $\times 100$, $\times 200$. The control sample, 40% ethanol solvent, was prepared in identical dilution series (\times 1, \times 5, $\times 10$, $\times 50$, $\times 100$, $\times 200$), respectively; all samples were made in triplicates (n = 3). According to the MTS test producer information (CellTiter 96 AQueous One Solution Cell Proliferation Assay, Promega, USA, [22]), if the cells are exposed to the test samples at the time when about approximately 70% "semi-confluent" cell culture had been occurred, the condition of the cytotoxicity study is accomplished; exposing the cells at the moment when 30% "sub-confluent" cell culture is done, the condition of the antiproliferative test is achieved. This way, Caco-2 cells are exposed to the test vegetal sample, control solvent sample, and control negative (blank) sample dilution series, of one cycle/24 h or two cycles/48 h of cell division, depending on the purpose of the study. Afterward, the culture medium was removed, and the cells were incubated with MTS solution for another 2 h. The absorbance (O.D.) at 490 nm of the test sample and solvent sample in comparison with the control negative (blank) sample is then recorded, and the viability of the adherent cells was calculated (Chameleon V Plate Reader, LKB Instruments). The results can be displayed as viability percent, or as O.D. at 490 nm along with the punctual concentrations in the series in the last case, also allowing the estimation of the solvent sample (40% ethanol) in the environment.

2.2.5 In silico computational studies

Anemonin and protoanemonin test ligands were prepared by energy minimization protocol using the Spartan'16 software [23,24]; the lowest conformers were employed for further docking simulations using CLC Drug, Discovery Work Bench (QIAGEN, Aarhus, Denmark). The four molecular targets selected for the study (COX-1, COX-2, TNKS1, and TNKS2) in combination with their native ligands were imported from Protein Data Bank (https://www.rcsb.org). They are PDB ID 3N8Y – the structure of COX-1 in complex with diclofenac [25]; PDB ID 1PXX: structure of (COX-2) in complex with diclofenac [26]; PDB ID 4W6E:TNKS1 with a small molecule inhibitor [27] and PDB 4HKI:TNKS2 in complex with flavan core [28]. The docking protocol involved the following steps: (a) ligand's preparation, (b) protein's preparation by protonation, (c) removal of co-factors and water molecules, (d) setup binding site and binding pocket, (e) docking simulations on co-crystallized and investigated ligands, (f) validation, (g) collecting property data, and (h) docking results. Interactions by hydrogen bonds of ligands within the active binding site of each target were identified and measured. Docking results were given in terms of docking score functions [29], and root-mean-square deviation (RMSD) values.

2.2.6 Equipment used

The instruments used for chemical analyses were UV/Vis spectrophotometer (Hélios γ , Thermo Electron Corporation, *U.K.*), and Linomat5 TLC visualizer (CAMAG, *Muttenz*, *Switzerland*). Pharmacological *in vitro* studies were done by xCELLigence DP Real-Time Cell Analysis (xC-RTCA) (ACEA Biosciences, *USA*).

3 Results and discussion

3.1 Analytical results

Qualitative high-performance thin-layer chromatography analysis first indicated a similitude of polyphenols fingerprint (Figure 2) in the two polar extracts, as results from the comparison of the aqueous extract An1 (Tracks T2) in chromatogram A with ethanolic extract An2/Tracks T4 in chromatogram B. *System A* setting study also revealed the "spring aspect" of the extracts, the dominance of polyglycosides and esterified forms, respectively. An1 and An2

(Tracks T4) extracts, both reveal the abundance of the highly esterified caffeic acid derivates (blue fluorescent/ fl. spots s0, s1, s4, s6, s7, s8, s9, s10), of quercetin polyglycosides (yellow-orange fl. spots s3, s5), as well as of apigenin derivates (dark green, fl. spot s2 and s11), aside from some smaller amounts of caffeic acid aglycone (blue, fl. spot s12) and ellagitannins (blue, fl. spot at the START positions of the chromatograms A and B, more augmented in the aqueous samples An1/Tracks T2). Allowing more detailed information about polyphenols aglycones in vegetal samples, System B setting study (chromatogram C) on the corresponding hydrolyzed samples, Track 7 (Anh1) in comparison with Track T9 (Anh2), both confirmed the presence of caffeic acid (s11) and quercetin (s8) aglycones, at the same time the occurrence of some methylated quercetin compounds namely (iso) rhamnetin derivates, punctually the yellow, yelloworange and light green fl. spots s10, s12, and s13; chromatogram C revealed vitexin (green fl. spot s6), and protocatechuic acid (blue-indigo fl. spot s9) presence as well. Literature data [1] also mention the presence of secondary metabolites in the class of (tri)terpenoids, volatile oils, alkaloids, lignans, and lactones in wood anemonederived products.

Chromatogram A: Track T1, rutin, chlorogenic, gallic, and caffeic acid (ref.); Track T2, *A. nemorosa* water extract An1 (duplicate sample); Chromatogram B: Track T3, rutin, vitexin, protocatechuic acid and apigenin (ref.); Track T4, *A. nemorosa* ethanolic extract An2 (duplicate sample); Track T5, hyperoside, cosmosiin, rosmarinic acid, kaempferol (ref.); Chromatogram C: Track T6, caffeic acid (ref.); Track T7, *A. nemorosa* water extract hydrolyzed sample Anh1;

Track T8, gallic acid (ref.); Track T9, *A. nemorosa* ethanolic extract hydrolyzed sample Anh2.

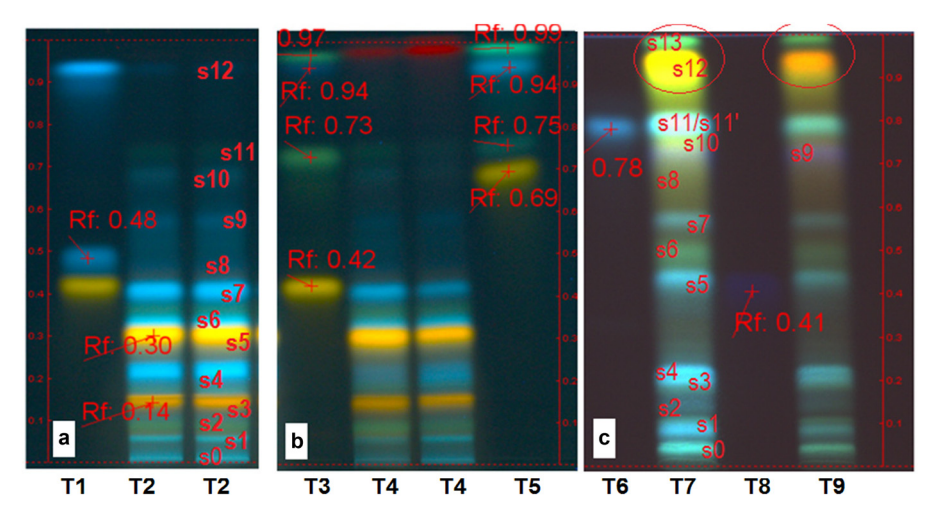


Figure 2: (HP)TLC studies on the polar extracts from A. nemorosa L.

Concerning quantitative aspects, the results indicated a slight superiority of polyphenols content in the ethanolic extracts, for example, starting from 50 g dried plant material (the aerial part of *A. nemorosa* L.), Anaq1 extract (300 mL) have revealed a content of 0.80 mg [GAE] per 1 mL sample thus summing 240 mg total phenols in the aqueous extract, while Anet2 extract (340 mL) have revealed a content of 0.74 mg [GAE] per 1 mL sample, therefore summing 251.60 mg total phenols in the ethanolic extract.

3.2 Antioxidant activity results

CL studies aimed to evaluate radical oxygen scavenger properties that the two polar extracts obtained from the dried wood anemone plant material. Studies have been done on the two standardized extracts, An1 and An2, prepared as identical 5 mg [GAE] per 1 mL 40% ethanol solvent, respectively. It must be reminded that according to the literature data presented [1–5], the dried plant material does not contain the unstable and volatile compound protoanemonin but a stable dimer compound anemonin.

Yet, antioxidant activity assay on the two test vegetal extracts, An1 and An2, face to the corresponding control (solvent) sample (ethanol 40%) indicated an augmented pro-oxidant activity (Figure 3), nearly twice (An1), and eight times (An2) stronger than that of the control sample (which contains $50 \, \mu L \, H_2 O_2 \, 10^{-3} \, M$).

Furthermore, IC₅₀ activity assay (Figure 4) on the An1 and An2 test vegetal samples (eight dilution series each one: $\times 10$, $\times 50$, $\times 100$, $\times 200$, $\times 300$, $\times 400$, $\times 500$, and

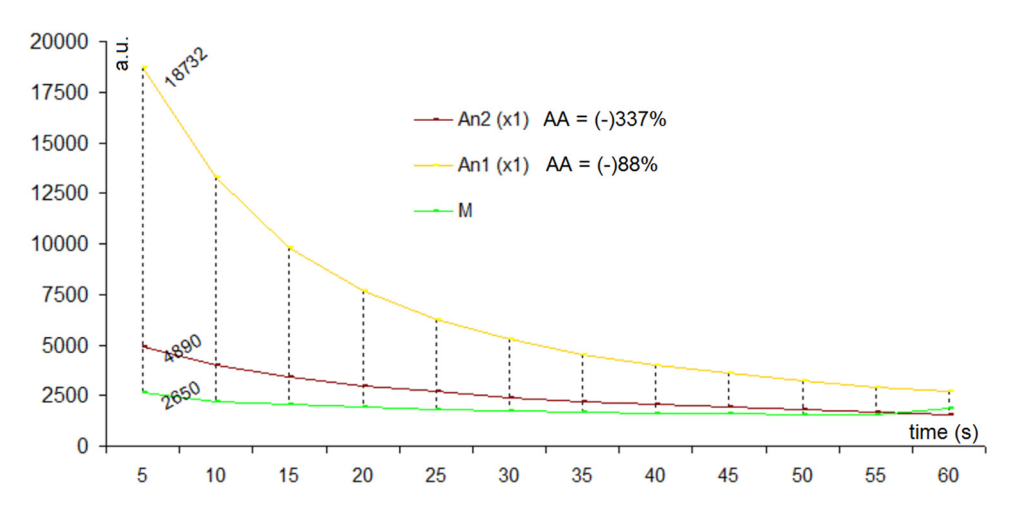


Figure 3: Antioxidant activity assay on the *A. nemorosa* L. polar extracts (An1, An2, dilution series $\times 1$), in comparison with the control sample (M, dilution series $\times 1$); n = 3.

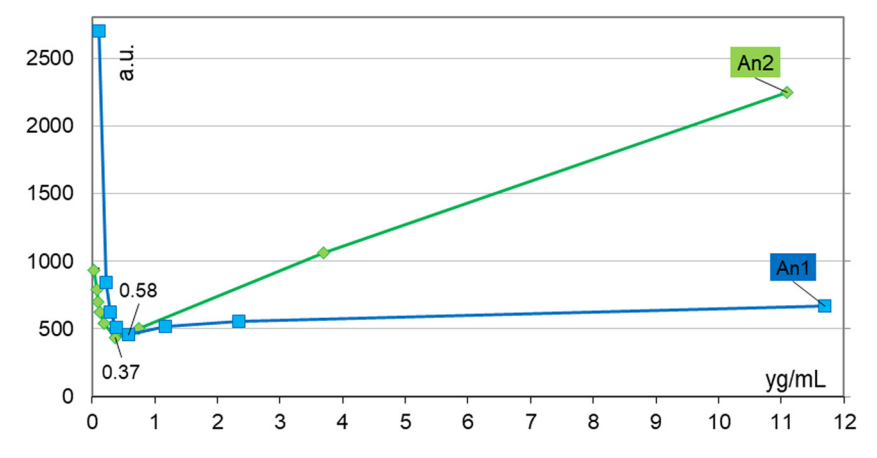


Figure 4: IC_{50} assay on the *A. nemorosa* L. extracts (An1, An2, eight dilution series, n = 6).

 \times 1,000, in 40% ethanol), foremost indicated the decrease of the pro-oxidant activity in the series toward the bottom value of the control sample, explained by the dilution of the pro-oxidant compounds in the samples. Afterward, both vegetal extracts have shown an unusual increased antioxidant activity, promptly in the interval $(\times10)-(\times300)$ in the case of An1, and in the interval $(\times10)-(\times100)$ in the case of An2, thus, in the concentration range between 0.1 and $10\,\mu g$ [GAE] per 1 mL sample, followed by another decrease of the antioxidant activity toward the maximum dilution points in the series $(\times1,000)$.

Data in Figure 4 also show the punctual IC₅₀ values of the test vegetal extracts: IC₅₀ = 0.290 μ g [GAE]/mL for An1, and IC₅₀ = 0.185 μ g [GAE]/mL for An2. Using identical CL testing method and solvents, gallic acid and rutin phenolic compounds (ref.) have computed with IC₅₀ values of 0.85 and 2.54 μ g/mL, respectively. The comparison with the reference compounds reveals the high antioxidant activity of the two polar extracts from *A. nemorosa* L. herba et flores dried plant material, particularly in the interval of 0.1 to 5 μ g [GAE] per 1 mL sample. At dilution points over 10 μ g [GAE] per 1 mL sample, both extracts from wood anemone have revealed an ascending pro-oxidant activity.

3.3 In vitro pharmacological activity results

Cytotoxicity and antiproliferative activity studies were also achieved on two standardized vegetal extracts (An1 and

An2), punctually in the concentration range including the highest antioxidant potency of the extracts in CL assay. MTS tests were done in comparison with the control solvent sample (40% ethanol, v/v), and control negative sample, on the Caco-2. The two test vegetal extracts, prepared as dilution series $\times 1$, $\times 5$, $\times 10$, $\times 50$, $\times 100$, and $\times 200$ (n=3), and the control solvent sample (40% ethanol) dilution series $\times 1$, $\times 5$, $\times 10$, $\times 50$, $\times 100$, and $\times 200$ (n=3) were applied at 24 and 48 h on the "semi-confluent" and "sub-confluent" Caco-2 cell cultures respectively, as described in the Section 2.2.4. The results were evaluated as O.D. at 490 nm along with μg total phenols per 1 mL sample, in comparison with the control negative samples series, to better emphasize the influence of the solvent in samples.

Figures 5–7 show the results on the cytotoxicity and antiproliferative MTS tests of the two test vegetal extracts (An1 and An2 dilution series) and the solvent sample control series (40% ethanol) in comparison with control negative test series; figures present O.D. at 490 nm along with a punctual concentration (μ g [GAE]) in samples, and also the percent (%, media value, n = 3) of the stimulatory and cytoprotective activity of test vegetal extracts.

Therefore, the cytotoxicity test at 24 h (Figure 5) indicated that both test vegetal extracts (An1 and An2) have provided a protective activity against 40% ethanol in medium (the solvent sample), and along with the entire concentration interval tested (from 0.05 to $10 \,\mu g$ [GAE]/1 mL sample); in the same time, An1 and An2 have revealed a stimulatory activity upon the viability of the Caco-2 cells in the interval between $0.1-2 \,\mu g$ [GAE]/1 mL sample. The

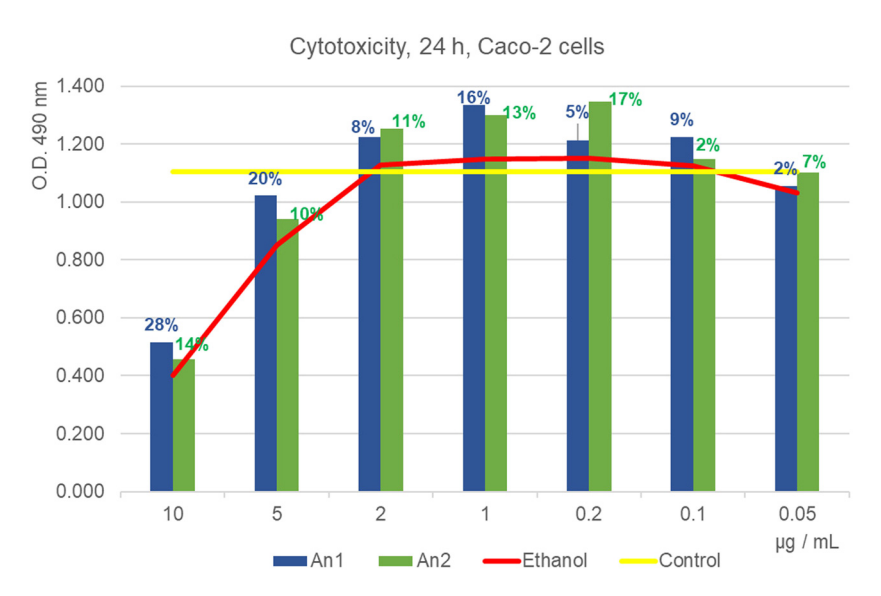


Figure 5: Caco-2 cell viability response after the treatment with the three-test sample (An1, An2, and 40% ethanol dilution series) in comparison with the control negative series, at 24 h.

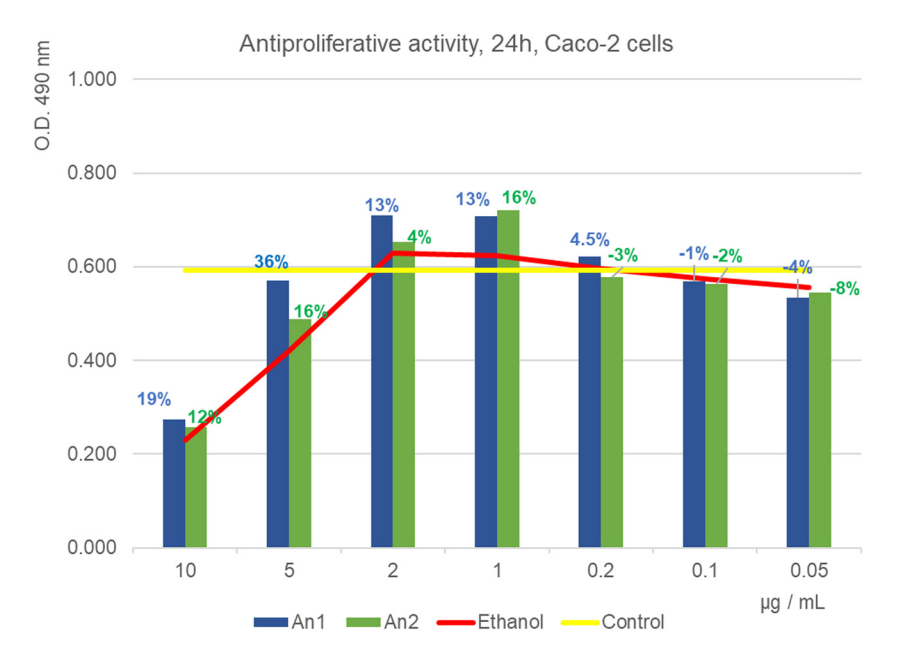


Figure 6: Caco-2 cell antiproliferative test response after the treatment with the three-test samples (An1, An2, and 40% ethanol dilution series) in comparison with the control negative series, at 24 h.

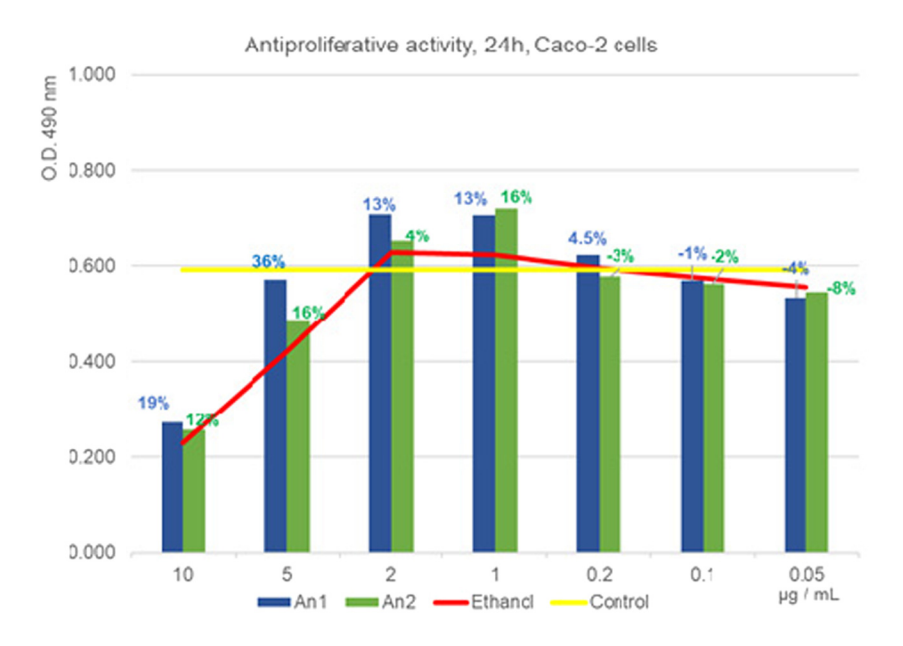


Figure 7: Caco-2 cell antiproliferative test response after the treatment with the three-test samples (An1, An2, and 40% ethanol dilution series) in comparison with the control negative series, at 48 h.

comparison with the solvent sample series (40% ethanol) indicated a stimulatory activity ranging from 2 to 28% in the case of An1, and from 2 to 17% in the case of An2.

The MTS antiproliferative test at 24 and 48 h, respectively (Figures 6 and 7), confirmed both aspects that were noticed in the MTS cytotoxicity test; the protective activity against 40% ethanol (in the interval 1-10 µg GAE per 1 mL sample), as well as stable stimulatory activity on the viability of Caco-2 in the interval 0.2-5 µg GAE per 1 mL sample; the intensity of the cell stimulation in comparison with the solvent sample series, 40% ethanol, 48 h after the two test vegetal extracts were applied on the Caco-2 cells, was estimated at 7-47% in the case of An1, and 9-19% in the case of An2.

Together, pharmacological studies proved simultaneously the protective and stimulatory activity of the high diluted aqueous and ethanolic extracts from the dried wood anemone plant material on Caco-2 cells. This stimulatory and protective activity was situated in the concentration area proved with the highest antioxidant potency in CL studies, also suggesting wood anemone extract's anti-inflammatory potential on the intestinal tissue.

In support, some in vitro studies on the transformed murine macrophage cell line RAW 264.7 have revealed the capacity of anemonin to inhibit the nitric oxide (NO). endothelin-1, and intercellular adhesion molecule-1 synthesis [30], three key mediators of the inflammatory process. In vitro studies have also shown the ability of anemonin to produce a selective decreasing of inducible nitric oxide synthase (iNOS) mRNA in the RAW 264.7 cell culture [30]. Since the iNOS overexpression is a nodal point in the inflammatory process and immune system response after lipopolysaccharide (LPS) stimulation in humans, and so as a nodal point in cardiovascular system diseases and arthritis development, it was further concluded that anemonin compound could be the basis of a new series of natural medicines targeting the iNOS reduction [31]. Anemonin also was confirmed with beneficial effects on the restoration of the intestinal barrier in LPS-challenged piglets in vivo; according to the data reported, the improvement in the mucosa recovery in LPS-challenged piglets was done through TGF-b1 and epidermal growth factor receptor pathways, by decreasing the expression of proinflammatory messenger's tumor necrosis factoralpha (TNF-α), and interleukins (IL)-6, IL-8, and IL-1beta [32].

Furthermore, similar to studies on Ranunculus species [33], the present studies have evidenced the presence of isorhamnetin derivates in hot water and hot ethanolic extracts from the aerial part of dried A. nemorosa L, as known (iso)rhamnetin derivates are assigned with a plethora of pharmacological activities including augmented anti-inflammatory properties. The anti-inflammatory mechanism of (iso)rhamnetin derivates comprised the control of the production of numerous inflammatory mediators (e.g., inhibition of COX-2 expression, inhibition of NF-kappa B signaling, a decrease of the expression of cytokines TNF alpha, IL-1 β, IL-6, IL-12, and matrix metalloprotease-1), and also of reactive oxygen species generation [34–41]. Furthermore, literature data [42] have revealed that isorhamnetin mitigates chemically induced inflammation in intestines (by activation of the nuclear receptor pregnane X receptor (PXR), by promotion of the upregulation of PXR-mediated metabolism of probiotics,

and by downregulation of NF-kappa B signal transduction), also suggesting high benefits in managing inflammatory bowel diseases in humans. Together, pharmacological studies *in vitro* and *in vivo* have revealed that anemonin and (iso)rhamnetin crossover similar biological activities, therefore they could have synergistic activity in achieving simultaneous stimulatory and protective activity on Caco-2 cells.

3.4 In silico results

Starting from the conclusions of the in vitro studies, which demonstrated the stimulatory potency of the polar extracts from wood anemone on the viability of the Caco-2, the question is whether the stimulatory effect is extended to the tumorigenesis process itself. Pharmacological studies along the time do not sustain a protumor activity, but they indicate an antitumor effect of the anemonin and wood anemone-derived products [4,34]. The present computational study aims to evaluate the interactions of the key compounds from wood anemone-derived products, anemonin, and protoanemonin, with two pairs of molecular targets involved in the inflammatory process and tumor development at the level of the intestinal tissue as well. The four molecular targets selected for the study were the two isoforms of the human cyclooxygenase (COX-1 and COX-2) known with a critical role in the inflammatory process [43,44], but also involved in the cancer development [45], and the two tankyrases in humans (TNKS1 and TNKS2).

In support, studies have shown that while COX-2 inhibition impedes the progress of the inflammatory process and pain symptoms in cancer disease, the inhibition of COX-1 enzyme could play an important role in managing ovarian, head, neck cancer, renal cell carcinoma, and hematological malignancy associated with high levels of COX-1 isoform [46]. TNKS1 and TNKS2 have also been involved in many types of cancer in humans; for example, it was counted that about 90% of the human colorectal tumors today present the hyperactivation of the β-catenin signaling pathway responding to the TNKS inhibitors [47]. Furthermore, TNKS1 and TNKS2 are considered today a "novel target for drug discovery [48]," since they have a crucial role in telomere regulation and other numerous biological processes, comprising "Wnt/β-catenin signaling pathway, viral replication, endogenous hormone regulation, glucose transport, cherubism disease, erectile dysfunction, and apoptosis [49]."

Finally, another molecular target to be considered for future prospecting studies on protoanemonin and anemonin is the human mitochondrial enzyme creatine kinase (MtCK); MtCK does not yet have a native ligand in PDB Bank, therefore, no estimates can be made of its effects. Known to "provide a temporal and spatial energy buffer to maintain cellular energy homeostasis [50], which acts as a mobile energy store available for regeneration of ATP at times of high demand," MtCK is considered a "prime therapeutic target in myocardial ischemia [51]," therefore a possible cause of the poisoning and deadly effect of protoanemonin, but also could offer the opportunity of studying new drugs targeting diseases by decreasing mitochondria energy (e.g., inflammatory bowel diseases, food intolerance).

The relevant results of docking studies on the four molecular targets in combination with their native ligands in PDB Bank, in comparison with the two natural ligands anemonin and protoanemonin in *Ranunculaceae*, in terms of hydrogen bond interactions, docking score, and RMSD, all together are presented in Tables 1–4.

In Table 1, results of simulations on cyclooxygenase-1 (PDB ID 3N8Y), bound to diclofenac, within the binding pocket setup at 61,44 Å³ are listed. The main finding is the involvement of TYR385 amino acid residue in hydrogen bonding with all the ligands, both the cocrystallized diclofenac and the studied ligands (anemonin and protoanemonin). This observation converges with the idea that TYR385 helps to stabilize the formation of cyclooxygenase-ligand complexes. According to the docking PLANTS_{PLP} score [32], negative score values are related to powerful binding affinities. Therefore, COX-1 docking study has revealed the following order in decreasing the bonding affinity of the ligands: diclofenac > anemonin > protoanemonin. Diclofenac is distinguished by the formation of two hydrogen bonds, both involving TYR385 amino acid residue, resulting in stronger stability of the complex COX-1-diclofenac. Anemonin and protoanemomin also interact by hydrogen bond formation with the same amino acid residue from COX-1' chain A, conducting to the conclusion of a moderate affinity and satisfactory inhibitory activity too.

Table 1: Results of molecular docking study on cyclooxygenase 1, COX-1 (PDB ID: 3N8Y, chain A, binding pocket at 61.44 Å³)

Ligand	Interacting group with 3N8Y, chain A	Hydrogen bonds: Å	Score/RMSD
Diclofenac	TRP387, PHE205, TYR385, LEU384, PHE381, MET522, GLY526, SER530, MET528, ILE523, LEU534, ALA527, GLU524, LEU531, ARG120, VAL116, TYR355, SER353, VAL349, VAL344, LEU532, TYR348, PHE518	O sp ² (O1)-O sp ³ TYR385: 2.677 O sp ² (O2)-O sp ³ TYR385: 2.528	-63.81/0.05
Anemonin	TYR348, TRP3878, TYR385, LEU384, SER530, GLY526, PHE518, MET522, ALA527, ILE523, MET525, GLU524, ARG120, TYR355, SER353, VAL349, LEU352	O sp ² (O2)-O sp ³ TYR385: 3.054	-38.95/0.004
Protoanemonin	TYR348, LEU352, PHE518, ALA527, ILE523, GLY526, MET522, SER530, PHE381, LEU384, TYR385, TRP387	O sp ² (O1)-O sp ³ TYR385: 3.54	-29.29/0.02

PBD ID: 3N8Y, chain A, binding pocket at 61.44 Å.

Table 2: Results of molecular docking study on cyclooxygenase 2, COX-2

Ligand	Interacting group/1PXX chain A	Hydrogen bonds: Å	Score/RMSD
Diclofenac	TYR355, SER353, LEU352, VAL349, TYR348, TRP387, SER530, TYR385, LEU384, PHE381, LEU525, PRO528, GLY526, MET522, VAL 523, ARG120, GLU524, ALA527, VAL523, PHE518, PHE518	0 sp ² -0 sp ³ SER530: 2.653 0 sp ² -0 sp ³ SER530: 2.905 0 sp ² -0 sp ³ TYR385: 2.729	-68.76/0.15
Anemonin	PHE205, TRP387, TYR385, LEU384, PHE381, SER530, LEU525, GLU524, ARG120, GLU524, ALA527, VAL523, MET522, TYR355, SER353, VAL349, LEU352, TYR348, VAL344, GLY526, LEU531	O sp ² -O sp ³ (-OH) TYR385: 2.547	-39.48/0.001
Protoanemonin	TYR348, LEU352, TRP387, TYR385, LEU384, PHE381, PHE518, SER530, VAL523, ALA527, GLU524, GLY526, MET522	O sp ² (O1)-O sp ³ TYR385: 2.87	-29.97/0.05

PDB ID: 1PXX, chain A, binding pocket at 78.34 Å³.

Table 3: Results of molecular docking study on human tankyrase 1, TNKS1

Ligand	Interacting group/4W6E, chain A	Hydrogen bonds: Å	Score/RMSD
3 5	MET1207, GLY1206, ILE1204, GLU1291, ALA1202, TYR1203, HIS1201, TYR1213, PHE1214, ALA1215, PHE1183, LYS1220, HIS1184, ILE1228, GLY1185, TYR1224, SER1185, PHE1188, PRO1187, LY1227, SER1121, ALA1290	O1 sp ³ -O sp ² GLU1291: 3.393 O1 sp ³ -O sp ² GLU1291: 3.250 O sp ² -O sp ³ SER1221: 2.778 O sp ² -Nsp ² GLY1185: 2.895	-104.15/0.16
Anemonin	LYS1220, SER1221, GLY1185, TYR1224, GLY1227, ILE1228, ARG1187, SER1186, HIS1184, TYR1213, TYR1203, HIS1201, ALA1202, GLY1211, ILE1212	NO hydrogen bonding	-41.45/0.0027
Protoanemonin	LYS1220, SER1221, TYR1224, GLY1185, HIS1184, PHE1183, ALA1215, ALA1290, GLU1291, TYR1213, TYR1203	O sp ² (O1)-N sp ² GLY1185: 2.671 O sp ² (O1)-O sp ³ SER1221: 2.933 O sp ² (O2)-O sp ³ SER1221: 3.118	-35.53/0.01

PDB ID: 4W6E, chain A, binding pocket at 140.29 Å³.

Table 4: Results of molecular docking study on human tankyrase 2, TNKS2

Ligand	Interacting group/4HKI, chain A and C	Hydrogen bonds: Å	Score/RMSD
FLN	LYS1067(A), SER1068(A), PHE1030(A), ALA1064(A), TYR1071(A), GLU1038(C), GLY1032(A), HIS1031(A), PHE1061(A), ILE1075(A), SER1033(A), PRO1034(A), TYR1061(A), PHE1035(A), HIS1048(A), ALA1049(A), TYR1050(A)	O sp ² (O4)-O sp ³ SER1068(A): 2.850 O sp ² (O4)-N sp ² GLY1032(A): 3.029	-76.97/0.02
Anemonin	LYS1067(A), SER1068(A), HIS1031(A), GLY1032(A), TYR1071(A), SER1023(A), PR01034(A), TYR1060(A), ILE1059(A), HIS1048(A), GLY 1058(A), ALA1049(A), GLY1074(A), ILE1075(A), TYR1050(A), ILE1051(A)	NO hydrogen bonding	-37.84/0.004
Protoanemonin	GLU1138(C), LYS1067(A), ALA1062(A), SER1068(A), PHE1030(A), GLY1032(A), HIS1031(A), TYR1071(A), PHE1061(A), TYR1060(A), TYR1050(A)	O sp ² (O1)-N sp ² GLY1032(A): 2.730 O sp ² (O1)-O sp ³ SER1068(A): 3.009 O sp ² (O2)-O sp ³ SER1068(A): 3.131	-35.58/0.02

PDB ID: 4HKI, chains A and C, binding pocket at 121.34 Å³.

In Table 2, are listed the docking results obtained on the crystal structure of COX-2 active site in complex with diclofenac. Similar results as in the case of COX-1 are shown. The docking score varies in the same way (in absolute values): diclofenac > anemonin > protoanemonin. Specifically, diclofenac forms three hydrogen bonds with two amino acids, TYR385 (chain A) and SER530, respectively. TYR385 is also involved in hydrogen bond interaction with oxygen atoms hybridized sp2 of anemonin and protoanemonin. Another observation is that the selectivity of the inhibition of COX-2 could also be achieved by designing compounds that interact with

SER530 only, avoiding TYR385 bond formation, which appears in COX-1-ligand formation only.

Schema of atoms labelling's for anemonin and protoanemonin compounds are given in the Supplementary Material (Figure S1); also, Figure S2 presents the results of the molecular docking study on COX-1 structure (PDB ID 3N8Y), while Figure S3 presents the results of the molecular docking study on COX-2 structure (PDB ID 1PXX), as resulted from Spartan's softwares computations for energy minimization.

Also, a similar behavior and explication is observed for anemonin, manifested by the absence of hydrogen bonding; Figure S4 presents the results of the molecular docking study on TNKS1 structure (PDB ID 4W6E), and Figure S5 presents the results of the molecular docking study on TNKS2 structure (PDB ID 4HKI).

Table 3 presents the complex formed by the molecular target TNKS1 and its native ligand, the cocrystallized 3J5; the results indicated great stability, resulting in a very high inhibitory score (-104.15). Specifically, four hydrogen bonds are formed: GLU1291, SER1221, and GLY1185 amino acid residues. Missing of hydrogen bond interactions but the presence of inhibitory effects could be explained with different types of contributions of heavyatom contacts (inter-atom distance less than 5.5 Å) between ligand and the binding site, other than hydrogen bond interactions, such as lone-pair-metal ion interactions, nonpolar interactions, nonpolar-polar contacts, repulsive contacts, evaluating the potential energy change at the formation of the protein-ligand complex [32]. Although the docking score for anemonin is higher, revealing the strongest binding affinity for protoanemonin, it can be noticed that no hydrogen interactions are present. By comparison, anemonin (-41.45) and protoanemonin (-35.53) were less active TNKS1 inhibitors, but more active than on COX isoforms; specifically, protoanemonin was proved with moderate inhibitory activity (-35.53), forming three hydrogen bonding, with the nitrogen atom of GLY1185 and oxygen sp3 of SER122. Also, similar behavior and explication are observed for anemonin, manifested by the absence of hydrogen bonding; Figure S4 presents the results of the molecular docking study on TNKS1 structure (PDB ID 4W6E), and Figure S5 presents the results of the molecular docking study on TNKS2 structure (PDB ID 4HKI).

Table 4 presents the interactions involved in the formation of TNKS2–ligands complexes; the complexes are due exclusively to GLY1032 and SER1068 amino acids residues from TNKS chain A. Also, the order of variation of the docking score is the same as in the case of TNKS1 complexes, but a moderate value of the binding affinity of the native ligand (FLN versus 3J5) is revealed.

4 Conclusion

Species in *Ranunculaceae* family are assigned with numerous pharmacological activities, protoanemonin, and anemonin being two of the key compounds. Other compounds with high biological activity in *A. nemorosa* plant species are polyphenolic compounds, such as caffeic acid esters and quercetin glycosides, including the methylated

forms namely (iso)rhamnetin derivates, while literature data also shown the presence of (tri)terpenoids, volatile oils, alkaloids, lignans, and lactones, thus adding some of the most active secondary metabolites in the green plants. Accordingly, pharmacological studies on the extracts and separate key compound anemonin all pointed out wood anemone-derived products stimulatory and/or protective activity on the viability and function of the cells from numerous tissues, for example, brain, heart, vessel, and intestinal tissue.

This study was designed to assess two polar extracts (An1/aqueous and An2/ethanolic) from wood anemone dried plant material in terms of polyphenols' profile, antioxidant activity, and cytotoxic and antiproliferative activity on the Caco-2. The selection of the Caco-2 cells was driven by the aim of prospecting *in silico* activity of anemonin and protoanemonin on several molecular targets associated with both, the inflammation process, and tumorigenesis in intestinal cells. The molecular targets selected for this purpose were the two human cyclooxygenases (COX1 and Cox2), and the two human tankyrases (TNKS1 and TNKS2).

CL studies on the two polar extracts from the wood anemone dried plant materials (An1 and An2 prepared as 5 mg [GAE] per 1 mL sample) indicated an augmented antioxidant activity in the concentration range from 0.1 to 5 μ g [GAE] per 1 mL sample; IC₅₀ values were 0.285 and 0.180 μ g [GAE] per 1 mL sample respectively.

In vitro cytotoxicity and antiproliferative MTS studies on An1 and An2 dilution series, both revealed simultaneous protective and stimulatory potency on the viability of the Caco-2 cells (viability increase up to 48%), specifically in the concentration area proved with the highest antioxidant potency (from 0.1 to 5 μ g [GAE]/1 mL sample).

In silico docking studies on the two key compounds in Ranunculaceae family, anemonin and protoanemonin, indicated their inhibitory activity on both, COX-1 and COX-2 activities, and TNKS1 and TNKS2 activities. Score activities of the two key compounds were analyzed in comparison with several native ligands, specifically, diclofenac in the case of COX enzymes, and flavan core and another small molecule native ligand found in PDB Data Bank in the case of TNKS enzymes. COX-1 and diclofenac (native ligand) indicated a strong interaction (score activity: -63.81) by two hydrogen bonds with the amino acid TYR385 (chain A), while the two test ligands (anemonin and protoanemonin) by one hydrogen bond each with TYR385 (chain A) had a moderate inhibitory activity (score activity: -35.95 and -29.29); COX-2 and diclofenac also achieved a strong interaction (score activity: -68.76)

by one hydrogen bond with TYR385 (chain A) and two hydrogen bonds with SER530, while anemonin and protoanemonin had moderate activity by one hydrogen bond each with TYR385 (chain A) only (score activity: -39.48 and -29.97). TNKS1 formed four very strong hydrogen bonds (score activity: -104.15) with the native ligand in PDB Data Bank (flavan core), two with GLU1291, one with SER1221, and one with GLY1185 amino acid residue; anemonin did not present hydrogen bonds but indicated a moderate inhibitory activity (score activity: -41.44) explained by the existence of other types of interactions with the amino acids in the active pocket, while protoanemonin established two hydrogen bonds with SER 1221 and another one with GLY1185 (score activity: -35.53). TNKS2 and the native ligand tested resulted in a strong interaction (score activity: -76.97) by one hydrogen bond with GLY1032 and two hydrogen bonds with SER1068 amino acid residues from chain A; similarly, anemonin did not present hydrogen bonds, but indicated moderate inhibitory activity (score activity: -37.84), while protoanemonin formed one hydrogen bond with GLY1032 and another one with SER1068, also resulting in moderate inhibitory activity (score activity: -35.58).

Summarizing, the concomitant protective and stimulatory activity on the viability of Caco-2, in the context of proving anemonin and protoanemonin inhibitory activity on four cell modulators related to inflammation and tumorigenesis processes in intestines, together suggest the usefulness of the wood anemone polar extracts in managing intestinal cell regeneration, specifically in post-operative recovery, and also in regenerative medicine by helping human cells, tissues, and organs to restore to normal function. A potential synergistic activity between anemonin, protoanemonin, and other COX and TNKS (native) ligands could be considered to the final effect of strengthening the inhibition of some major mediators of inflammation and tumorigenesis in humans.

Funding information: This study is financed through the Ministry of Research, Innovation and Digitization ROMANIA, Program NUCLEU 2019. Grant number: PN 19-41.

Author contributions: conceptualization – Lucia Pirvu; methodology – Lucia Pirvu and Georgeta Neagu; formal analysis – Lucia Pirvu, Georgeta Neagu and Amalia Stefaniu; investigation – Lucia Pirvu, Georgeta Neagu, Amalia Stefaniu and Lucia Pintile; writing and original draft preparation – Lucia Pirvu and Amalia Stefaniu; project administration – Lucia Pirvu and Amalia Stefaniu; funding acquisition – Amalia Stefaniu. All the authors

have accepted responsibility for the entire content of this submitted manuscript and approved submission.

Conflict of interest: The authors declare no conflicts of interest regarding this article.

Ethical approval: The conducted research is not related to either human or animal use.

References

- [1] Turner N. Counter-irritant and other medicinal uses of plants in Ranunculaceae by native peoples in British Columbia and neighbouring areas. J Ethnopharmacol. 1984;11(2):181–201.
- [2] Dalefield R. Poisonous plants. Veterinary Toxicology for Australia and New Zealand. 1st edn.. Masterton, New Zealand: Elsevier; 2017.
- [3] Guil-Guerrero JL. The safety of edible wild plants: fuller discussion may be needed. J Food Compos Anal. 2014;35(1):18-20.
- [4] Hao D-C, Gu X, Xiao P. Anemone medicinal plants: ethnopharmacology, phytochemistry and biology. Acta Pharm Sin B. 2017;7(2):146-58.
- [5] Hill R, Van Heyningen R. Ranunculin: the precursor of the vesicant substance of the buttercup. Biochem J. 1951;49(3):332-5.
- [6] Schrenk D, Merz K-H, Jochims K. Feasibility study of nonclinical safety assessments on homeopathic preparations using the example of protoanemonin in Pulsatilla pratensis L. Regul Toxicol Pharmacol. 2013;66(1):104–8.
- [7] Dr Willmar Schwabe India Anemone Nemorosa Dilution 200 CH, Dr Willmar Schwabe India Anemone Nemorosa Dilution 200 CH. Available from: https://www.1mg.com/otc/dr-willmar-schwabe-india-anemone-nemorosa-dilution-200-ch-otc396131.
- [8] Erickson RO, Rosen GU. Cytological effects of protoanemonin on the root tip of Zea Mays. Am J Bot. 1949;36(4):317–22.
- [9] Rosca MG, Hoppel CL. Mitochondrial dysfunction in heart failure. Heart Fail Rev. 2013;18(5):607-22.
- [10] Baer H, Holden M, Seegal BC. The nature of antibacterial agent from Anemone pulsatilla. J Biol Chem. 1946;162:65–8.
- [11] Holden M, Segal BC, Baer H. The range of antibiotic activity of protoanemonin. Proc Soc Exp Biol Med. 1974;66(1):54-60.
- [12] Mares D. Antimicrobial activity of protoanemonin, a lactone from ranunculaceous plants. Mycopathologia. 1987;98(3):133-40.
- [13] Martín ML, San Román L, Domínguez A. In vitro activity of protoanemonin, an antifungal agent. Planta Med. 1990:56(1):66-9.
- [14] Jia D, Han B, Yang S, Zhao J. Anemonin alleviates nerve injury after cerebral ischemia and reperfussion. J Mol Neurosci. 2014;53:271–9.
- [15] Lukianchuk A, Khropot O, Konechnyi Y, Konechna R, Novikov V. Wood anemone. Anemone nemorosa L. Analytical review. ScienceRise Pharm Sci. 2017;3(7):38-42.
- [16] Huang Y-H, Lee T-H, Chan K-J, Hsu F-L, Wu Y-C, Lee M-H. Anemonin is a natural bioactive compound that can regulate

- tyrosinase-related proteins and mRNA in human melanocytes. J Dermatol Sci. 2008;49(2):115-23.
- [17] Romanian Pharmacopoeia. Xth edn. Bucharest: Medicala; 1993.
- [18] Wagner H, Bladt S. Plant drug analysis. A thin layer chromatography atlas. 2nd edn. Berlin Heidelberg: Springer-Verlag; 1996.
- [19] Reikh E, Schibli A. HPTLC for the analysis of medicinal plants. Thieme NY: Stuttgart; 2008.
- [20] Pirvu L, Hlevca C, Nicu I, Bubueanu C. Comparative studies on analytical, antioxidant, and antimicrobial activity on a series of vegetal extracts prepared from eight plant species growing in Romania. J Planar Chromatogr. 2014;27(5):346-56.
- [21] Meghea A, Iftimie N, Giurginca M. The estimation of the antioxidant effect of plants extracts by chemiluminescence. Rev Chim. 2004;55(12):1025-8.
- [22] Protocols & Applications Guide. Available from: https://www. promega.ro/ (accessed on 2 August 2021).
- [23] Shao Y, Molnar LF, Jung Y, Kussmann J, Ochsenfeld C, Brown ST, et al. Advances in methods and algorithms in a modern quantum chemistry program package Advances in methods and algorithms in a modern quantum chemistry program package. Phys Chem Chem Phys. 2006;8:3172-91.
- [24] Hehre WJ. A guide to molecular mechanics and quantum chemical calculations. Irvine, CA: Wavefunction Inc.; 2003.
- [25] Sidhu RS, Lee JY, Yuan C, Smith WL. Comparison of cyclooxvgenase-1 crystal structures: cross-talk between monomers comprising cyclooxygenase-1 homodimers. Biochemistry. 2010;49(33):7069-79.
- [26] Rowlinson SW, Kiefer JR, Prusakiewicz JJ, Pawlitz JL, Kozak KR, Kalgutkar AS, et al. A novel mechanism of cyclooxygenase-2 inhibition involving interactions with Ser-530 and Tyr-385. J Biol Chem. 2003;278(46):45763-9.
- [27] Johannes JW, Almeida L, Barlaam B, Boriack-Sjodin PA, Casella R, Croft RA, et al. Pyrimidinone nicotinamide mimetics as selective tankyrase and wnt pathway inhibitors suitable for in vivo pharmacology. ACS Med Chem Lett.
- [28] Narwal M, Haikarainen T, Fallarero A, Vuorela PM, Lehtio L. Screening and structural analysis of flavones inhibiting tankyrases. J Med Chem. 2013;56(9):3507-17.
- [29] Korb O, Stutzle T, Exner TE. Empirical scoring functions for advanced protein-ligand docking with PLANTS. J Chem Inf Model. 2009;49(1):84-96.
- [30] Duan H, Zhang Y, Xu J, Qiao J, Suo Z, Hu G, et al. Effect of anemonin on NO, ET-1 and ICAM-1 production in rat intestinal microvascular endothelial cells. J Ethnopharmacol. 2006;104(3):362-6.
- [31] Lee TH, Huang NK, Lai TC, Yang ATY, Wang GJ. Anemonin, from Clematis crassifolia, potent and selective inducible nitric oxide synthase inhibitor. J Ethnopharmacol. 2008;116(3):518-27.
- [32] Xiao K, Cao ST, Jiao LF, Lin FH, Wang L, Hu CH. Anemonin improves intestinal barrier restoration and influences TGF-B1 and EGFR signaling pathways in LPS-challenged piglets. Innate Immun. 2016;22(5):344-52.
- [33] Bhatti MZ, Ali A, Ahmad A, Saeed A, Malik AM. Antioxidant and phytochemical analysis of Ranunculus arvensis L. extracts. BMC Res Notes. 2015;8:279. doi: 10.1186/s13104-015-1228-3.

- [34] Gong G, Guan Y-Y, Zhang Z-L, Rahman K, Wang S-J, Zhou S, et al. Isorhamnetin: a review of pharmacological effects. Biomed Pharmacother. 2020;128:110301.
- [35] Li W, Chen Z, Yan M, He P, Chen Z, Dai H. The protective role of isorhamnetin on human brain microvascular endothelial cells from cytotoxicity induced by methylglyoxal and oxygen-glucose deprivation. J Neurochem. 2016;136(3):651-9.
- [36] Zhao JJ, Song JQ, Pan SY, Wang K. Treatment with isorhamnetin protects the brain against ischemic injury in mice. Neurochem Res. 2016;41(8):1939-48.
- [37] Yang B, Li X-P, Ni Y-F, Du H-Y, Wang R, Li M-J, et al. Protective effect of isorhamnetin on lipopolysaccharide-Induced acute lung injury in mice. Inflammation. 2016;39(1):129-37.
- [38] Li Y, Chi G, Shen B, Tian Y, Feng H. Isorhamnetin ameliorates LPS-induced inflammatory response through downregulation of NF-kB signaling. Inflammation. 2016;39(4):1291-301.
- [39] Li J, Wu R, Qin X, Liu D, Lin F, Feng Q. Isorhamnetin inhibits IL-1β-induced expression of inflammatory mediators in human chondrocytes. Mol Med Rep. 2017;16(4):4253-8.
- [40] Jaramillo S, Lopez S, Varela LM, Rodriguez-Arcos R, Jimenez A, Abia R, et al. The flavonol isorhamnetin exhibits cytotoxic effects on human colon cancer cells. J Agric Food Chem. 2010;58(20):10869-75.
- [41] Kim SY, Jin C-Y, Kim CH, Yoo YH, Choi SH, Kim G-Y, et al. Isorhamnetin alleviates lipopolysaccharide-induced inflammatory responses in BV2 microglia by inactivating NF-kB, blocking the TLR4 pathway and reducing ROS generation. Int J Mol Med. 2019;43(2):682-92.
- [42] Dou W, Zhang J, Li H, Kortagere S, Sun K, Ding L, et al. Plant flavonol isorhamnetin attenuates chemically induced inflammatory bowel disease via a PXR-dependent pathway. J Nutr Biochem. 2014;25(9):923-33.
- [43] Smith WL, Garavito RM, DeWitt DL. Prostaglandin endoperoxide H synthases (cyclooxygenases) -1 and -2. J Biol Chem. 1996;271(52):33157-60.
- [44] Fitzpatrick FA. Cyclooxygenase enzymes: regulation and function. Curr Pharm Des. 2004;10(6):577-88.
- [45] Miciaccia M, Belviso BD, Iaselli M, Cingolani G, Ferorelli S, Cappellari M, et al. Three-dimensional structure of human cyclooxygenase (hCOX)-1. Sci Rep. 2021;11(1):4312.
- [46] Perrone MG, Scilimati A, Simone L, Vitale P. Selective COX-1 inhibition: a therapeutic target to be reconsidered. Curr Med Chem. 2010;17(32):3769-805.
- [47] Haikarainen T, Krauss S, Lehtio L. Tankyrases: structure, function and therapeutic implications in cancer. Curr Pharm Des. 2014;20(41):6472-88.
- [48] Lehtio L, Chi N-W, Krauss S. Tankyrases as drug targets. FEBS J. 2013;280:3576-93.
- [49] Damale MG, Pathan SK, Shinde DB, Patil RH, Arote RB, Sangsheti JN. Insights of tankyrases: a novel target for drug discovery. Eur J Med Chem. 2020;207:112712.
- [50] Schlattner U, Tokarska-Schlattner M, Wallimann T. Mitochondrial creatine kinase in human health and disease. Biochim Biophys Acta. 2006;1762(2):164-80.
- [51] Whittington HJ, Ostrowski PJ, McAndrew DJ, Cao F, Shaw A, Eykyn TR, et al. Over-expression of mitochondrial creatine kinase in the murine heart improves functional recovery and protects against injury following ischaemia-reperfusion. Cardiovasc Res. 2018;114(6):858-69.